Updated charts of the mean annual wind stress, convergences in the Ekman Layers, and Sverdrup transports in the North Atlantic

by Ants Leetmaa[1] and Andrew F. Bunker[2]

ABSTRACT

From the wind stress computation of Bunker (1976) for the North Atlantic, the annual mean and seasonal vertical velocities which result from convergences in the Ekman Layers are computed. Charts of the geostrophic and total transport (geostrophic plus Ekman) are constructed using the Sverdrup relationship. Of particular interest are an intense current leaving the coast at the point where the Gulf Stream separates and a cyclonic gyre north of the Stream in this area. Good agreement exists between the computed features of the large scale circulation patterns and the observed ones. Close correspondence exists between the predicted and observed paths of the Gulf Stream; separation from the coast occurs at the maxima in the wind stress.

1. Introduction

As part of a larger investigation to estimate the total energy flux between the ocean and the atmosphere, wind stress distributions were computed by one of us for the North Atlantic Ocean (Bunker, 1976). In recent years a number of authors have constructed charts of the curl of the wind stress in order to estimate large scale ocean transports (Hantel, 1971, Evenson and Veronis, 1975, and Bye, Noye, and Sag, 1975). Since this computation has been done several times recently, the question arises as to why it should be repeated yet again.

Saunders (1976) estimated the annual wind stress in 1° squares over a 10° square in the North Atlantic. Using these values in estimating the curl of the stress, he found that the value of the curl can be greatly underestimated if it is based on 5° square wind stress data. Thus in the previous studies which used that spatial resolution, the curl of the stress, and consequently the ocean transports, were probably underestimated. For the present study, in most areas the stress was computed over areas 2° of latitude × 5° of longitude. This spacing still is larger than the one employed by Saunders. However, most of the spatial variation in the stress occurs in the meridional direction; consequently the lack of resolution in the zonal direction

1. National Oceanic and Atmospheric Administration, Atlantic Oceanographic and Meteorological Laboratories, Miami, Florida, 33149, U.S.A.
2. Woods Hole Oceanographic Institution, Woods Hole, Massachusetts, 02543, U.S.A.

is not a major drawback in computing the net meridional transports across the whole ocean basin along a latitude circle, and based on Saunders study 2° resolution in latitude should be sufficient.

Comparison of the geostrophic transport at several latitudes in the North Atlantic, as estimated from hydrographic data, with the transport estimated using the curl of the stress from Bunker's (1976) calculation in the Sverdrup relation, shows quite good agreement (Leetmaa, Niiler and Stommel, 1977). This comparison provides some evidence that the present estimates are probably reasonably accurate. They may perhaps be still a bit low because of the limited resolution. It would require a much more ambitious effort to redo these calculations on a finer grid. Even then there are regions such as large areas of the Southeastern Atlantic where the data base is insufficient for reliable estimates of the stress on the finer grid.

2. The observations and error estimates

The National Climatic Center (NCC) has collected weather reports and sea surface temperatures from ships, converted them to uniform formats, eliminated gross errors, and recorded them on magnetic tape. This series of data, designated TDF-11, is described in a notebook by NCC. Data from 66 Marsden Squares (10° squares) for the years 1941-72 were obtained from NCC and processed for the present study. Nearly 12 million reports were read from the tapes. Of these about 4 million reports were rejected, primarily because observations of one or more variables were missing. A computer program was written to check the quality of each report, select the reports with all the variables necessary, compute energy fluxes, and form averages of fluxes. The bulk aerodynamic equations were used to compute the stresses. Drag coefficients were used which vary with wind speed and stability. A complete discussion of the choice of drag coefficients and the computational procedures is given in Bunker (1976).

There are three major sources of error in estimating the wind stress (Bunker, 1976). The first is possible errors in the estimation of the wind. Ship reports are the source of most of the wind observations. Previous investigations have shown that median winds are underestimated by marine vessels relative to weather ships by about 5%. The choice of a value for a drag coefficient adds another 10-20% uncertainty into the stress computation. Additional uncertainty results from inadequate spatial resolution of the wind stress field. The data used in the curl computations usually were averaged over regions measuring 2° of latitude by 5° of longitude. Near coasts and over large areas where little data were available the stresses were averaged over irregularly shaped areas. A spatially centered finite difference scheme was employed to estimate the curl operator where Δx was 10° of longitude and Δy was 4° of latitude. The curl computation was not done in the areas next to the coast. Where Bunker's (1976) data were over irregular shaped areas, these were averaged to areas 2° by 5°. In the region in which Saunders (1976) did his com-

putation, our curl estimates differ from his, averaged to our areas, by ± 30% for the 2° × 5° areas. Additional zonal averaging to areas 2° × 10° reduces this difference to a minus 5 to 10%, i.e. our estimates are lower than his. The larger errors for the smaller averaging region reflect the fact that there is structure in the meridional winds on a scale of less than 5°. This, of course, does not affect the net meridional transport which is a sum over the width of the basin and averages over this structure. Thus the smaller error estimate is the appropriate one. Thus, possible underestimation of the wind speed, uncertainty in the choice of a drag coefficient, and inadequate spatial resolution contribute to an overall uncertainty in our curl computation of about 30%.

3. Mean charts

Contours of the mean annual zonal and meridional wind stress are shown in Figure 1. The largest values of the stress tend to be in the zonal direction. Maxima in the east-west stress occur off the east coast of the United States, off Newfoundland, and at about 55N and 25W. These tend to lie over the boundary between warm and cold water that is defined by the Gulf Stream. Another maximum occurs in the region of the Trade Winds centered near 15N, 50W. The magnitude of the meridional wind stress is generally much less than that of the zonal stress. Large maxima in the meridional stress do occur, however, off the west coast of Africa and south of Greenland. These charts show larger values by about 25-50% of the stress for the maxima and more spatial structure for the maxima than Hellerman's (1968) (as depicted in Evenson and Veronis, 1975).

Using these mean values for the wind stress, the quantity $\text{curl}_z\ (\vec{\tau}/f)$ was computed from $\text{curl}\ z(\vec{\tau}/f) = \frac{\partial}{\partial x}(\tau_y/f) - \frac{\partial}{\partial y}(\tau_x/f)$, where $\vec{\tau} = (\tau_x, \tau_y)$ is the wind stress, $f = 2\Omega \sin \Theta$ is the Coriolis parameter, Ω is the angular velocity of the earth's rotation, and Θ is the latitude. This quantity represents the divergence of the Ekman transport, i.e. the vertical velocity times the density at the base of the ocean Ekman layer, i.e. the net divergence in this layer. Under certain assumptions it is equal to β/f times the total meridional geostrophic transport in the ocean (see Stommel (1965), pp. 154-156, for a discussion about the relationship between the curl of the stress, Ekman convergences, Sverdrup transport, and geostrophic transports). The computations were carried out between 5N and 60N. Close to the equator, it is not clear what the dynamical balances in the near surface boundary layer are. Thus it is not appropriate to use the present formalism to compute the convergence. The regions close to the continental boundaries were also omitted because of possible boundary effects on the dynamics. The results for the mean value of the vertical velocity at the base of the Ekman layer are shown in Figure 2.

One thing to note is that the values are larger than have been reported previously

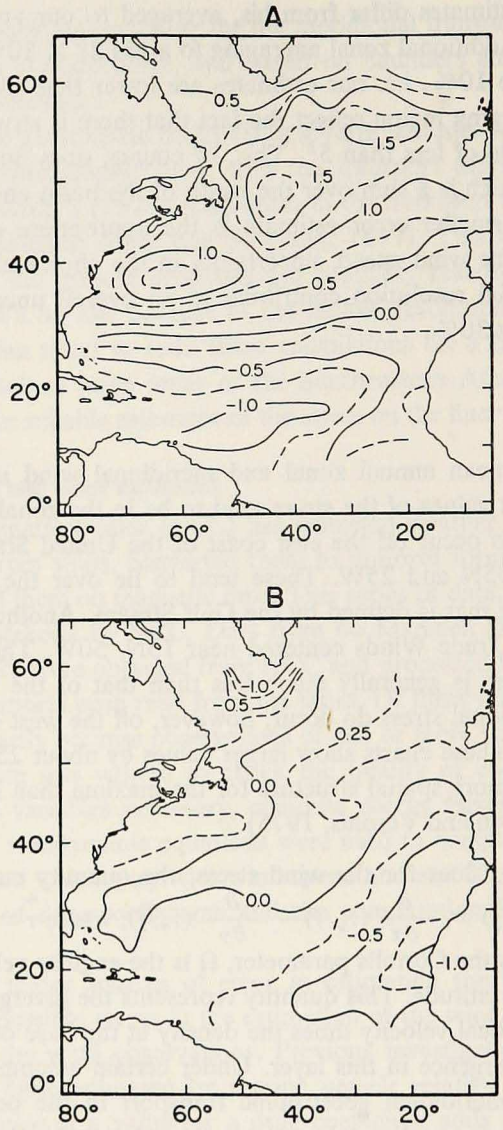

Figure 1. A) Contours of annual mean eastward wind stress over the North Atlantic. Units are dynes/cm^2.
B) Contours of annual mean northward wind stress. Units are dynes/cm^2.

(see, for example, Stommel (1964)). The zero line which separates the subpolar (vertical velocity positive) from the subtropical (vertical velocity negative) gyres follows the maxima in the eastward component of the wind stress. The subpolar gyre consists in fact of two gyres—one off the east coast of America and the other

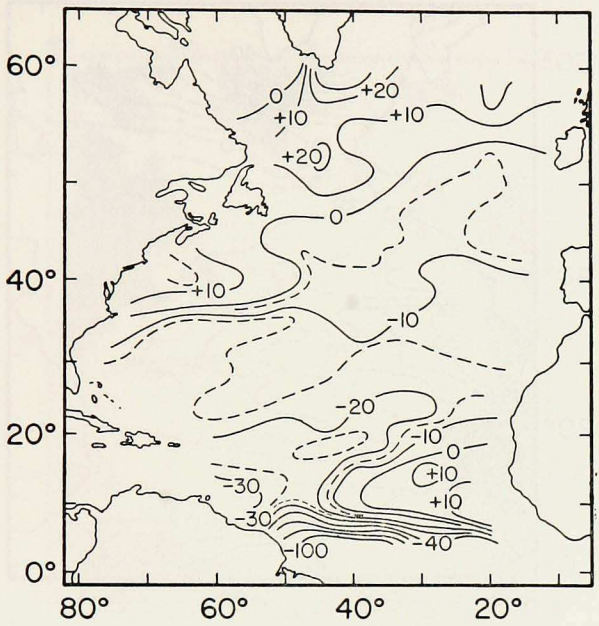

Figure 2. Annual mean vertical velocity at base of Ekman layer. Positive is upward. Units are 10^{-5} cm/sec. Note that off South America the contours between −60 and −100 are left out because of crowding.

north of about 50N. Another region of positive vertical velocities appears off the African coast.

Contours of the Sverdrup mass transport stream function are shown in Figure 3. These were determined by computing first in each 2° × 5° box the meridional Ekman and geostrophic transports. Then starting at the eastern boundary, where the transport function is assumed to be zero, the net meridional transport (Ekman plus geostrophic) at every 5° of longitude is obtained by summing westward. The resulting field is then contoured. The calculated total southward transport at 31N is 32 × 10^{12} g/sec. This is comparable to what is observed to flow northward through the Florida Straits (Leetmaa, et al. 1977). An interesting feature about the distribution of the predicted transport is an intense current that leaves the coast at the latitude that the Gulf Stream is observed to separate from the coast. The maximum in the wind stress that overlies this region is related to the intense winter storms. To the north of this maximum the curl is positive. An oceanic cyclonic gyre whose transport is 10-15 × 10^{12} g/sec, is driven by the positive curl if topographic effects are not important. Perhaps this gyre is related to the observed slope water circulation. Below 12°C slope water is indistinguishable in its *T-S* properties from water in the Gulf Stream. Consequently its transport and the deep recirculation on the Sargasso side of the Stream as postulated by Worthington (1976) com-

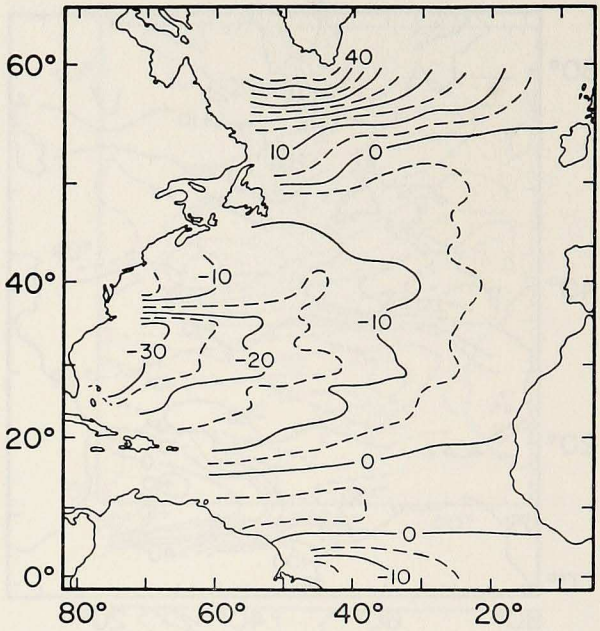

Figure 3. Contours of the annual mean Sverdrup mass transport. Units are 10^{12} g/sec.

plicate the problem of determining the wind-driven contribution to the total measured Gulf Stream transports in this area.

North of about 50N the curl is predominantly positive. This drives a subpolar gyre that has a maximum transport of about 40 Sverdrups. A gyre with comparable transports was derived by Evenson and Veronis (1975). At 59N between 10W and 20W the northward wind-driven flow is about 10×10^{12} g/sec.; this possibly continues into the Norwegian Sea. Worthington (1970) from direct measurements estimated the inflow to be about 8×10^{12} g/sec. However, he postulated that this was driven by thermohaline processes occurring in the Norwegian Sea and not the curl of the stress.

The total transport map (Fig. 3) indicates that by continuity there should be a northward flow (Brazil Current?) along the coast of Brazil to about 5N. However, between 16N and 5N the total transport along the coast in the boundary current should be southward. The Ekman transports in the interior are to the north and greater than the predominantly southward geostrophic transports. Thus the net interior flow is to the north and this results in a southward transport along the coast in the boundary current. This picture of the total transport agrees with the circulation pattern in this area as deduced from the T-O_2 correlations by Metcalf and Stalcup (1967). They concluded that the Brazil Current extends northward only to 5N because between there and 16N water with low oxygen content, associated with

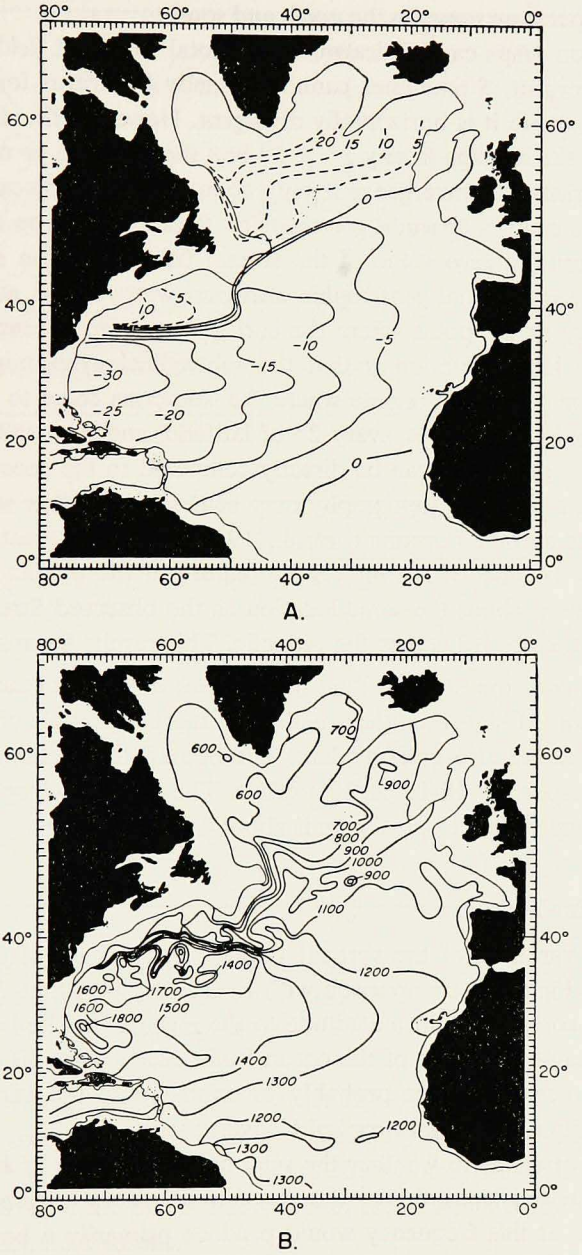

Figure 4. A) Contours of annual mean geostrophic volume transport. Units are 10^{12} g/sec. B) Chart of dynamic topography of 100 db surface relative to 1500 db surface in dynamic meters $\times 10^3$.

temperatures between 13° and 24°C, lies between water with higher oxygen content in this same temperature range to the north and south.

Stream function maps can be drawn for the total transport field since it is horizontally non-divergent. Streamlines cannot formally be drawn for the geostrophic transport field because it is horizontally divergent. However, the divergence is generally small. On the average in any 2° × 5° box the flux into or out of the Ekman layers due to horizontal convergence is only about 5% of the geostrophic transport in that box. This enables "pseudo-geostrophic" streamlines to be constructed. This is done by assuming a zero value of the stream function at the eastern boundary and summing the meridional geostrophic transport westward 5° at a time until the western boundary *or* the point where the curl goes to zero is reached. A rationale for choosing the latter criterion is that the subtropical gyres might be separated from the subpolar gyres by a regime where the isotherms come to the surface. This westward summation is done at every 2° of latitude, and then the resulting field is contoured. This construction can be directly compared to the geostrophic flow field as deduced from a dynamic topography map of the 100 decibar surface relative to the 1500 decibar surface (Leetmaa, et al., 1977). There is great visual similarity between Figures 4A and B. An interesting feature in the predicted flow field is a concentrated flow in about the same location as the observed Stream from 35N to 50N flowing northeastward across the Atlantic. This results because the zero of the curl of $(\vec{\tau}/f)$ lies over the Stream. That it continues to do so all across the Atlantic is rather surprising. Using this construction of the geostrophic transport field the two cyclonic gyres are also quite evident. The one off the east coast of the United States has a transport of 10-15 × 10^{12} g/sec. The total geostrophic transport between this gyre and the subtropical gyre is about 45 × 10^{12} g/sec.

4. Seasonal fluctuations

The seasonal variation of the vertical velocity at the base of the Ekman layer, W_e, is shown in Figure 5. Comparison with Figure 2 shows that the fluctuations in most places are comparable in magnitude to the mean W_e. The largest fluctuations tend to be on the western side of the ocean basin except near 10N. There they extend across the ocean and are probably associated with the annual cycle in the strength and position of the Intertropical Convergence.

The question arises as to whether the seasonal fluctuations in W_e can be related to fluctuations in the transport of the western boundary currents. Theoretically, fluctuating winds at this frequency would produce primarily a barotropic response (see discussion in Evenson and Veronis, 1975). On the other hand, the *mean* Sverdrup transport seems primarily to be concentrated in the upper ocean (Leetmaa, Niiler, Stommel, 1977). Also, most of the evidence about seasonal fluctuations is from hydrographic measurements and only gives information about fluctuations in

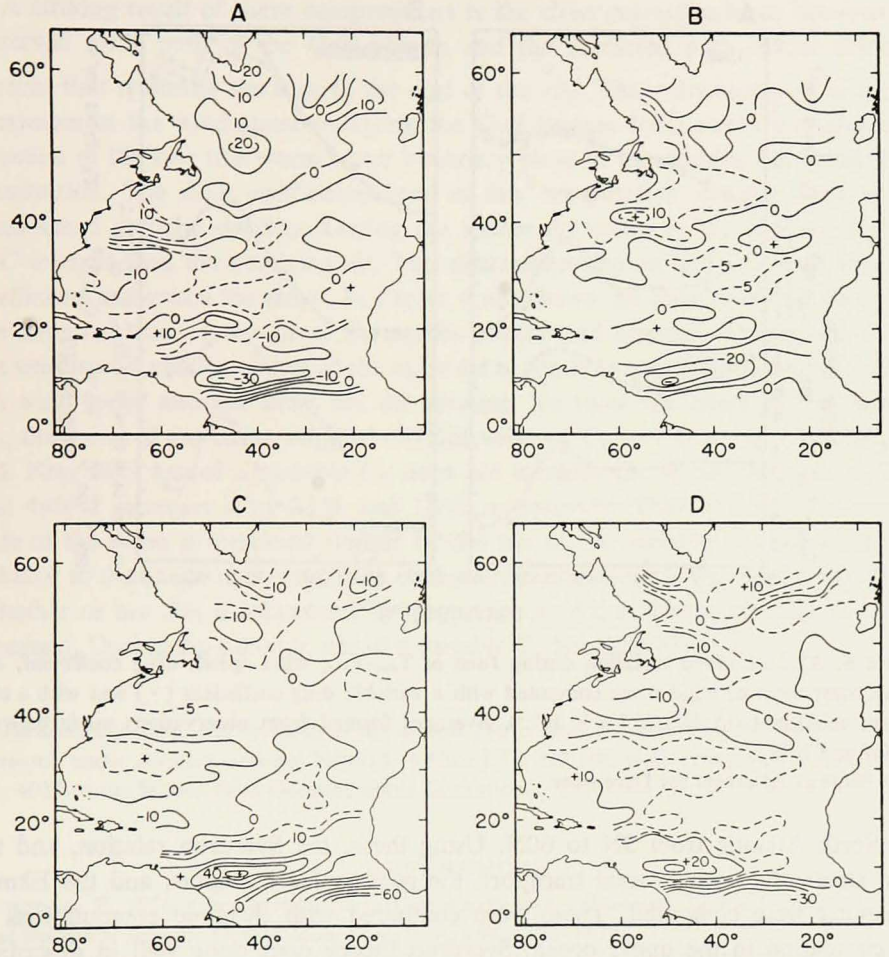

Figure 5. Graphs of the seasonal vertical velocity minus the annual mean vertical velocity at the base of the Ekman layer. Units are 10^{-6} cm/sec.
A) Winter B) Spring C) Summer D) Fall.

the baroclinic transport. So instead of presenting detailed maps of the seasonally varying Sverdrup transport, we presently report only the transports at 31N. These are in units of 10^{12} g/sec: winter, 48; spring, 38; summer, 26; fall, 17. The fluctuations are about 50% of the mean value. Direct measurements are needed to verify the existence of such fluctuations.

5. Discussion

From the recent wind stress computations of Bunker (1976), the mean and seasonally varying vertical velocity at the base of the Ekman layer were computed for

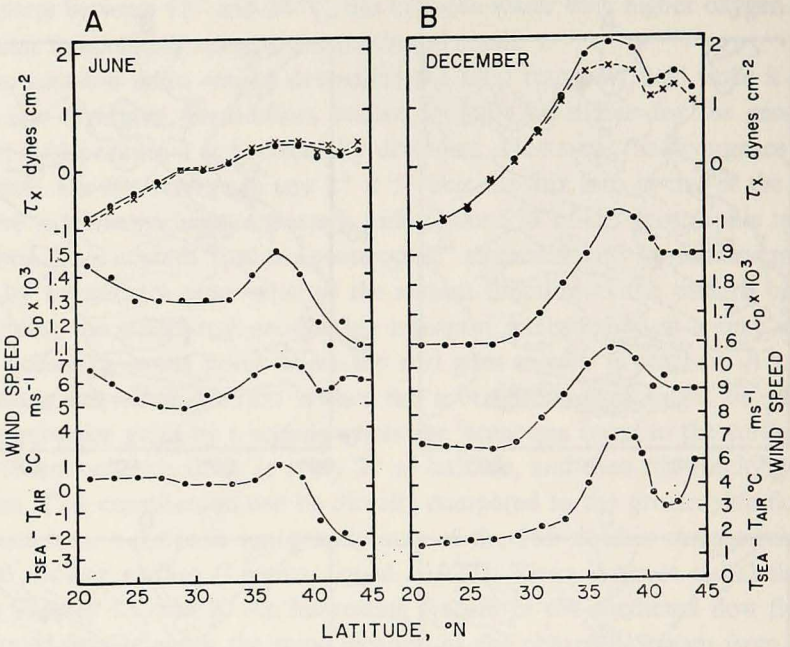

Figure 6. A) Latitudinal variation during June of T_{sea}-T_{air}, wind speed, drag coefficient, and east component of wind stress computed with a variable drag coefficient (•) and with a constant coefficient (x), ($C_D = 1.6 \times 10^{-3}$). Averages formed from observations made between 65W and 70W.

B) Same as A) except for December.

the North Atlantic from 5N to 60N. Using these, the Sverdrup relation, and the wind stress, the oceanic total transport, the geostrophic transport, and the Ekman transports were computed. These were compared with dynamic computations of the circulation in the upper ocean. Sverdrup theory does quite well in describing the horizontal distribution of these transports. The computations, however, still fail to account for the large observed transports in the Gulf Stream after it leaves the coast. Observations show this to be an area with intense eddy activity. It is possible that higher order dynamics involving inertial effects, bottom influences, or the eddies can explain the increased transport.

Munk's (1950) estimate of the total southward transport was 36×10^{12} g/sec. A value based on Hellerman's more recent stress computations is 24×10^{12} g/sec. The present computations give a value of 32×10^{12} g/sec. It is remarkable that despite better data, higher spatial resolution, and improved values of the drag coefficient the results have not changed a lot. However, examination of the wind stress distribution Munk used indicates that his estimates of the mean stresses were perhaps too high. Further comparison of such computations to the general circulation is also limited because there are insufficient direct observations of deep transports.

A striking result of these computations is the close correspondence between the observed mean path of the Gulf Stream and the predicted path of the eastward current that underlies the zero in the curl of the $\vec{\tau}/f$. This coincidence of a narrow maximum in the wind stress overlying the Gulf Stream front raises the interesting question of the role this warm water boundary plays in determining the wind stress distribution. The drag coefficients used in this computation are functions of the wind speed and the stability. During the winter the water in the Stream is about 7°C warmer than the overlying air. This destabilizes the air and increases the drag coefficient and hence the stress. In Figure 6 are shown the quantities that enter into the determination of the stress during the winter and summer. During the winter the wind speed and instability of the air work *in* phase to maximize C_D at 37° where the wind speed and the stress are the greatest. To show the effect of the variable C_D, the value of the stress using a constant value of $C_D = 1.6 \times 10^{-3}$ is also plotted. Near 30N use of a variable C_D does not increase the stress; whereas, at 37N and 44N it increases it by 25% and 18% respectively. Thus although the magnitude of the stress is increased slightly by the use of the variable C_D, the main contributor to the shape and magnitude of the stress maximum is the wind speed itself. Whether or not this is influenced by the presence of the Stream remains to be determined. During the summer, use of a variable C_D has little effect.

Acknowledgments. The research of the second author was supported by the Office of Naval Research under contract number N00014-74-C0262.12; NR 083-004. This paper is contribution No. 4023 of the Woods Hole Oceanographic Institution.

REFERENCES

Bunker, A. F. 1976. Computation of surface energy flux and annual air-sea interaction cycles of the North Atlantic Ocean. Mon. Wea. Rev., *104,* 1122–1139.

Bye, J. A., B. J. Noye, and T. W. Sag. 1975. A monthly analysis of global wind stress and the ocean transports predicted from a numerical model. Quart. J. R. Met. Soc., *101,* 749–762.

Evenson, A. J. and G. Veronis. 1975. Continuous representation of wind stress and wind stress curl over the world ocean. J. Mar. Res., *33,* 131–144.

Hantel, M. 1971. Wind stress curl—the forcing function for oceanic motions, *in* Studies in Physical Oceanography, a tribute to Georg Wust on his 80th birthday. A. H. Gordon, ed., New York; Gordon and Breach, 124–136.

Hellerman, S. 1967. An updated view of the wind stress on the world ocean. Mon. Wea. Rev., *95,* 607–626. Corrigenda 1968, Ibid., *96,* 63–74.

Leetmaa, A., P. Niiler, and H. Stommel. 1977. Does the Sverdrup relation account for the Mid-Atlantic circulation? J. Mar. Res., *35,* 1–9.

Metcalf, W. G., and M. C. Stalcup. 1967. Origin of the Atlantic Equatorial Counter Current. J. Geophys. Res., *72,* 4959–75.

Munk, W. H. 1960. On the wind-driven ocean circulation. J. Meteor., *7,* 79–93.

Saunders, P. M. 1976. On the uncertainty of wind stress curl calculations, J. Mar. Res., *34,* 155–160.

Stommel, H. 1964. Summary charts of the mean dynamic topography and current field at the surface of the ocean, and related functions of the mean windstress. Studies in Oceanography, K. Yoshida, ed., Seattle, University of Washington Press, 568 pp.

—— 1965. The Gulf Stream, University of California Press, Berkeley. 248 pp.

Sverdrup, H. V. 1947. Wind-driven currents in a baroclinic ocean; with application to the equatorial currents of the eastern Pacific. Proc. Nat. Acad. Sci. Wash., *33,* 318–326.

Worthington, L. V. 1970. The Norwegian Sea as a Mediterranean Basin. Deep-Sea Res., *17,* 77–84.

Worthington, L. V. 1976. On the North Atlantic circulation. Johns Hopkins Oceanographic Studies, *6,* 110 pp.

Received: *5 October, 1977;* revised: *13 February, 1978.*